Advances in Concrete Construction, *Vol. 10, No. 2 (2020) 105-111*
DOI: https://doi.org/10.12989/acc.2020.10.2.105

Shear strength and deformation of steel fibre-reinforced concrete beams after fire

Antonius*[1], Rinda Karlinasari[1a], Purwanto[2b] and Aref Widhianto[1c]

[1]Department of Civil Engineering, Universitas Islam Sultan Agung, Semarang, Indonesia
[2]Department of Civil Engineering, Universitas Semarang, Semarang, Indonesia

(*Received June 15, 2019, Revised July 13, 2020, Accepted July 23, 2020*)

Abstract. In this study eleven beam of steel fibre-reinforced concrete were tested on concentrated load in order to evaluate the shear strength and deformation of the beams after burning. Variables considered in the test include spaces of shear reinforcement (stirrups) and temperature (normal temperature at 38°C, 300°C, 600°C and 900°C). The steel fiber used is set at 0.5% of the concrete volume. The phenomenon of the test results shows that although the beams were tested to achieve shear failure, the fact that all the tested beams did not encounter any shear failure. It has shown the influence of steel fibers and stirrups that plays a role in determining the mode of collapse. The concrete shear capacity of steel fibrous concrete beams installed with stirrups in altered spacing variations is not significantly different from each other, while beam deformability increases when the space stirrups are reduced. Furthermore, models of the developed-steel fibrous shear strength are compared and discussed with experimental results.

Keywords: shear; ductility; beams; steel fiber; stirrups; temperatures

1. Introduction

Nowadays concrete technology is developing so rapidly. Since concrete has both a high crack strength and ductile nature therefore it becomes the main goal of innovation in the development of concrete materials. One of the prominent developments is the development of high-strength concrete (HSC) which has been able to produce concrete compressive strength of more than 100 MPa. However, HSC has so brittle nature that its ductility is low. To overcome this condition, particularly in the case of HSC columns, it is necessary to confine adequate cross section of the concrete core (Paultre *et al.* 2010, Antonius *et al.* 2017). Another alternative to improve ductility in concrete materials is by adding fibre to the concrete mixture (Barros *et al.* 2013, Han *et al.* 2015). The application of fibrous concrete especially steel fibrous concrete continues to grow as of today due to durable and very ductile nature, include the mechanical behaviour after fire (Ponikiewski *et al.* 2018). Structurally, steel fibrous concrete has also been developed such as for prestressed concrete (Tadepalli *et al.* 2015) or panel structure (Luo and Vecchio 2016). In line with ongoing research, the thermal nature of fibre steel has also been comprehensively investigated, and proposed as constitutive models of steel fibrous concrete at high temperatures (Antonius *et al.* 2014, Blesak *et al.* 2016). However, the design equation for steel fibrous concrete has not been regulated based on Indonesian concrete standards (SNI-2847-2013).

ACI 544 1988 and Araujo *et al.* (2014) explained that the addition of the volume of the steel fibre fraction would either reduce the crack width in the concrete or increase the shear capacity even though the minimum volumetric stirrups ratio was used. Even steel fibrous concrete beams installed with stirrups will be able to control cracks and to minimize penetration of cracks into the compressive zone. The shear failure mode that usually occurs in plain concrete beams will change to a flexible collapse mode if the concrete beam contains steel fibers (Kwak *et al.* 2002, Yoon *et al.* 2017, Gomes *et al.* 2018). Lamide *et al.* (2016) also revealed that the sliding capacity of steel fibre self-compacting concrete (SFSCC) was 40% higher than the normal shear capacity of concrete beams. Meanwhile, Lim and Hong (2016) explained that the shear strength of very high strength steel fibrous concrete beams (f'_c>100 MPa) was higher than the predicted shear strength based on the design equation in the standard (ACI 318-14).

However, Jain and Singh (2013) stated that the shear strength of concrete beams containing steel fibers with a volume fraction of only 0.5% was lower than the predicted shear strength based on ACI 318-14. ACI 318-14 requires whether the ultimate shear strength value (V_u) is greater than half of the factored concrete cross section shear capacity ($0.5\phi V_c$) then shear reinforcement with a spacing of at least $0.5d$ is needed, where d is the distance from the tensile reinforcement centroid to the compressed-concrete fibers. Based on the problems described above, the shear

*Corresponding author, Professor
E-mail: antonius@unissula.ac.id
[a]Lecturer
E-mail: rkarlinasari@gmail.com
[b]Ph.D. Student
E-mail: purwanto_sipilusm@yahoo.com
[c]Assistant
E-mail: arefwdh@gmail.com

ISSN: 2287-5301 (Print), 2287-531X (Online)

Table 1 Models of shear strength of steel fibre concrete

Authors	Shear strength equation
Sharma (1986)	$v_{fc} = \frac{2}{3} f_t'(d/a)^{0.25}$ $f_t' = 0.79(f_c')^{0.5}$
Narayanan *et al.* (1987)	$v_{fc} = e\left[0.24 f_{spfc} + 80\rho\frac{d}{a}\right] + v_h$ $f_{spfc} = \frac{f_{cuf}}{(20-\sqrt{F})} + 0.7 + 1.0\sqrt{F}$ F is fibre factor $(L_f / D_f)V_f d_f$
Ashour *et al.* (1992)	$v_{fc} = (0.7\sqrt{f_c'} + 7F)\frac{d}{a} + 17.2\rho\frac{d}{a}$ The equation for *a/d*<2.5
Kwak *et al.* (2002)	$v_{fc} = 3.7e(f_{spfc})^{2/3}\left(\rho\frac{d}{a}\right)^{1/3} + 0.8v_b$ $e = 3.4\frac{d}{a}$ for $\frac{a}{d} \le 3.4$ $v_b = 0.41TF$ $TF = 4.15$ *MPa*

Note: The above shear strength equation is in MPa units

strength according to the above ACI can be achieved, the concrete beam containing minimum steel fibers which is 0.5%, needs to be combined with the strength of stirrups which are installed as a unit of steel fiber-reinforced concrete beams.

The purpose of this research was to evaluate the beams installed stirrups containing steel fibrous fraction of 0.5%. The parameters considered in the test; 100, 150 and 200 mm spaced stirrups (s), the temperature (T) refers to a beam at normal temperature (38°C), then burned at 300°C, 600°C and 900°C. The shear strength and deformability of steel fibrous concrete beams at elevated temperatures are the main objectives of this study. The proposed models will be validated with the results of this experiment.

2. Shear strength of steel fibre-reinforced concrete

The ultimate shear strength of steel fibre-reinforced concrete beams is the sum of plain concrete shear strength (V_c), shear strength due to the influence of fibers (V_f) and stirrup shear strength (V_s) which is written as follows

$$V_u = V_c + V_f + V_s \tag{1}$$

If the concrete and steel fiber is mixed into one concrete mixture accordingly the superposition of the first and second terms on the right hand side of Eq. (1) will be steel fibrous concrete (V_{fc}) or can be written

$$V_{fc} = V_c + V_f \tag{2}$$

Therefore Eq. (1) develops into

$$V_u = V_{fc} + V_s \tag{3}$$

If the stirrups used in the beam is placed upright, the shear strength of stirrups is as follows

$$V_s = A_v . f_y . \frac{d}{s} \tag{4}$$

Fig. 1 Steel fibre

In recent years there have been a lot of proposals for the shear strength of steel fibre concrete models developed by the researchers as shown in Table 1. The equation proposed by Sharma (1986) was revealed through research on the effect of steel fibers on shear strength by testing seven SFRC beams with concrete compressive strength (f'_c) was about 45 MPa. The test results showed that steel fibers were effective in enhancing the shear strength of SFRC beams and crack capacity was higher than the crack capacity of plain concrete. The proposed model by Narayanan and Darwish (1987) was developed through shear testing of forty-nine SFRC beams with compressive strength ranges between 40-80 MPa. Some parameters examined in this test comprise the presence and absence of shear reinforcement and fibre ratio (V_f).

The proposed model by Ashour *et al.* (1992) is an evaluation of the testing of eighteen HSFRC beams with 93 MPa concrete compressive strength where beam specimens are installed with or without stirrups. The tested parameters include *a/d* ratio, longitudinal reinforcement ratio and volume of fibre fraction. The test results indicated that the beam shear strength increased when the fibre volume fraction increased too. The shear strength equation based on Kwak *et al.* (2002) is basically the development of the equations of shear strength proposed by Narayanan. Furthermore, the equation is elaborated based on the testing of normal strength concrete beam specimens (f'_c~30 MPa) and high strength concrete (f'_c~68 MPa). The parameters examined included fibre volume fraction (V_f=0; 0.5; 0.75%) and the ratio *a/d* (the distance between the centered load and the support of the beam height from the compressive area to the center of the tensile reinforcement).

3. Experimental program

Eleven reinforced concrete beam specimens containing 0.5% fibre fraction volume with dimension of 100×200×600 mm were made in the experimental program. The used steel fibers has a ratio of length to diameter between 45 and 50 (Fig. 1). The installed longitudinal reinforcement has a low ratio of 0.96%. Parameters considered are stirrups with a diameter of 6 mm with space variations (s) of 100, 150 and 200 mm or 0.61d, 0.91d and 1.22d. The space of stirrups used are all above the maximum spacing provisions based on ACI 318-14 (0.5d). Stirrups yield stress is obtained from the steel tensile test and yield stress value (f_y) of 290 MPa. Another parameter is normal temperature at (38°C), 300°C, 600°C and 900°C.

Table 2 Relationship between time and burning temperature

Time (minutest)	Temperature (°C)
0	38.8
10	124.6
20	219.1
27	300
30	332.2
40	426.3
50	517.1
58	600
60	621.4
70	719.7
80	831.3
85	900
90	957.4

Fig. 2 Combustion process

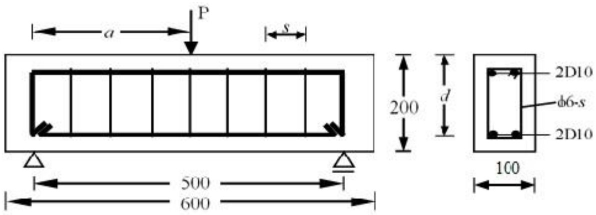

Fig. 3 Details of specimens and cross section (unit in mm)

The concrete mix plan refers to SNI 7656:2012 while the burning process of test specimens refers to the method used by Antonius *et al.* (2019). The temperature in the empty combustion chamber is considered the same as the temperature at the testing period. The temperature that occurs can be seen in the temperature measuring device installed in the combustion chamber, namely the thermocouple. Thermocouples are placed right in front of the fire that spurts from the blower. When there is no combustion, temperature readings are carried out using a multimeter. When it is read 38 on multimeter it means that the temperature in the combustion chamber before the combustion takes place is around 38°C. Based on temperature testing in the combustion process, the relationship between the length of time needed to reach this temperature and the combustion temperature is obtained. The relationship between time and combustion temperature can be seen in Table 2.

Based on Table 2 above, it takes a 27 - minute burning time to attain a temperature of 300°C. While for a 58 and 85-minute consecutive combustion, the temperatures achieved are 600°C and 900°C, respectively. Fig. 2 shows the combustion process of the test object.

Fig. 4 Testing the beam to collapse

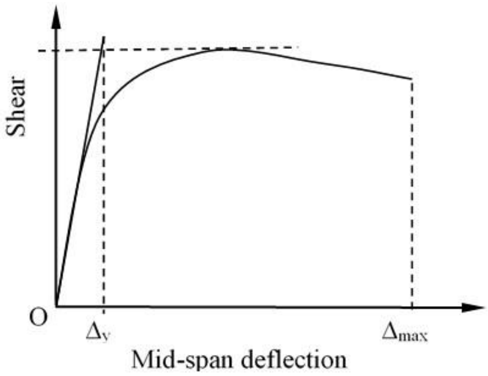

Fig. 5 Ductility definiton

The beams were tested against the load centered in the middle of the span with a displacement-control testing system. Centralized load and the length of the beams are arranged in such a way that the *a/d* ratio is 2.4 (see Fig. 3). Loading on the beams was directly applied at certain intervals until the beam collapsed in which at each increment of the load was directly correlated with the deflection of the beam in the middle of the spans. The beam testing mechanism is shown in Fig. 4.

The test results will be processed into a curve of the relationship between shear forces to the mid-span deflection (Δ) for all specimens. In evaluating the deformation ability of the specimens, ductility parameter (μ) is used and defined according to Fig. 5, meanwhile the ductility calculation is shown in Eq. (5).

$$\mu = \frac{\Delta_{max}}{\Delta_y} \tag{5}$$

4. Experimental results and discussion

Table 3 shows the experimental results of the eleven specimens tested. Δ_{max} value is taken from the maximum deflection of the beam in the middle of the span. $V_{exp.}$ value is the shear force capacity in support, and $v_{exp.}$ is the shear stress (unit MPa) resulting from the value of V_{exp} divided by multiplication between the width of the beam (b) with the value (d). The total shear stress value of each specimen (v_u) is also predicted based on the proposed models in Table 1 above added by the shear force of stirrups for each specimen (Eq. (3)).

Table 3 Experimental results

Specimen	T (°C)	s (mm)	f_c' (MPa)	V_f (%)	Δ_{max} (mm)	$V_{exp.}$ (kN)	μ	$v_{exp.}$ (MPa)	v_u (MPa) Sharma	Narayanan	Ashour	Kwak
B1	38	100	55.9	0.5	25.76	67.5	8.3	4.12	5.18	4.72	5.70	5.93
B2	300		38.1		15.26	65.75	5.2	4.01	4.14	3.82	4.68	4.80
B3	600		28.4		15.5	63.4	5	3.87	3.65	3.47	4.20	4.30
B4	900		23.8		14.3	59.1	4.6	3.60	3.37	3.27	3.92	4.02
B5	38	150	55.9		19.2	65.9	5.7	4.02	4.64	4.18	5.15	5.38
B6	300		38.1		19.46	62.85	5.7	3.83	3.74	3.41	4.27	4.40
B7	600		28.4		16.69	62.18	4.9	3.79	3.29	3.09	3.82	3.92
B8	900		23.8		8.92	58.33	2.6	3.56	3.02	2.92	3.57	3.66
B9	38	200	55.9		17.13	67.5	4.6	4.12	4.37	3.90	4.88	5.11
B10	600		28.4		14.68	62.95	3.9	3.84	3.09	2.90	3.64	3.73
B11	900		23.8		8	57.93	2.2	3.53	2.84	2.74	3.39	3.49

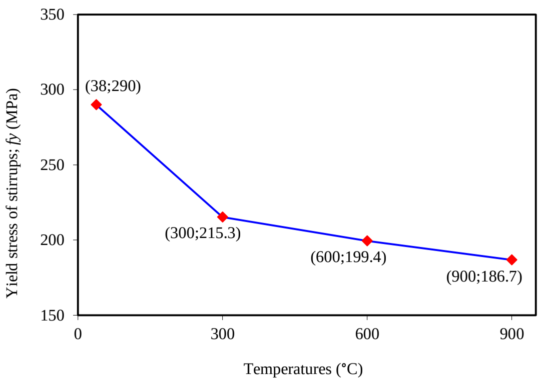

Fig. 6 Yield stress of stirrups at elevated temperatures

The compressive strength of steel fibrous concrete (f'_c) is produced from a cylindrical test of 150x300 mm and shows that at normal temperatures the value of f'_c is 55.9 MPa. Value f'_c has decreased to 38.1 MPa at 300°C, 28.4 MPa at 600°C and becomes 23.8 MPa if the cylinder is burned at 900°C. On the other hand after all post-fuel specimens were tested, stirrups from the beams were taken and tested to get the actual yield stress value at each temperature. As mentioned in the description of the experimental program above, the yield stress of stirrups at normal temperature is 290 MPa. After the specimen is burned and tested, the stirrups are taken then a tensile test is performed to determine the actual yielding stress after burning. The yield stress of stirrups from the tensile test results is shown in Fig. 6 where at a temperature of 300°C the f_y value is 215.3 MPa, at a temperature of 600°C the f_y value drops to 199.4 MPa and at 900°C the value of f_y drops again to 186.7 MPa. The actual yield stresses of these stirrups are used in calculating the shear strength of stirrups at each temperature.

(a) B1, T=38°C (flexural failure)

(b) B2, T=300°C (flexural failure)

(c) B3, T=600°C (diagonal tension failure)

(d) B4, T=900°C (diagonal tension failure)

Fig. 7 Failure mode of specimen, s=100 mm

(a) B5, T=38°C (flexural failure)

(b) B6, T=300°C (flexural failure)

(c) B7, T=600°C (flexural failure)

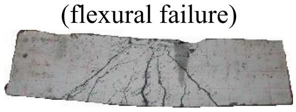

(d) B8, T=900°C (diagonal tension failure)

Fig. 8 Failure mode of specimen, s=150 mm

(a) B9, T=38°C (flexural failure)

(b) B10, T=600°C (diagonal tension failure)

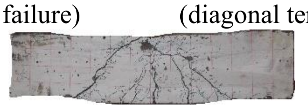

(c) B11, T=900°C (diagonal tension failure)

Fig. 9 Failure mode of specimen, s=200 mm

4.1 Failure modes

The collapse mode of all specimens is shown in Figs. 7-9. The loading process imposed on the beam is carried out in stages from starting to zero load until a crack occurs in the middle of the span. Loading continues until cracks propagate to the surrounding along with increasing load. In all specimens, the propagation process of the initial crack took place almost the same and there was no indication of shear failure. Several specimens have a type of flexural mode (B1, B2, B5, B6, B7, B9), and other specimens encounter diagonal tension failure mode (this happened when specimens were heated in higher temperature and the space of stirrups were expanding at the same time). Although the used steel fiber is only 0.5%, the contribution of steel fiber combined with the installation of stirrups is still able to prevent the beam from experiencing shear failure.

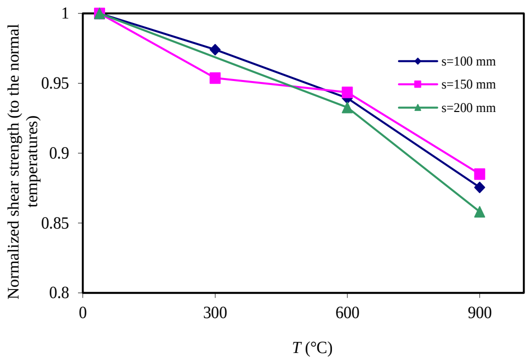

Fig. 10 Effect of spacing of stirrups to the ultimate shear strength at elevated temperatures

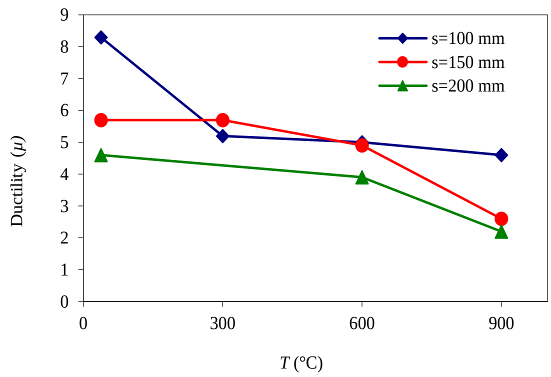

Fig. 12 Effect of spacing of stirrups to the ductility at elevated temperatures

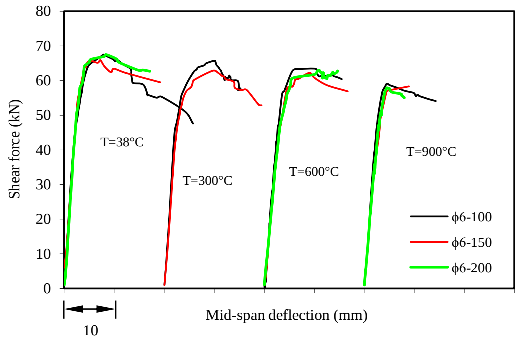

Fig. 11 Shear force vs mid-span deflection with various of spacing of stirrups

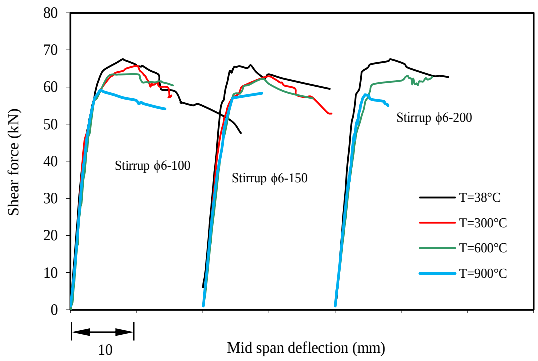

Fig. 13 Shear force vs mid-span deflection behavior with various of temperatures

4.2 Shear strength and deformation

4.2.1 Shear strength

Fig. 10 shows the curve of the relationship between the specimen shear strength normalized to the shear strength of the specimen at normal temperature, where at each temperature the spacing of stirrups are not the same for each specimen. Seen in Table 3 and Fig. 10, spacing stirrups are not very influential in determining shear strength. For example in specimens that were burned at a temperature of 300°C, the shear strength between specimens having spacing of 100 mm stirrups and 150 mm differed only by 3%. The shear strength among specimens with stirrups mounted with spaces 100, 150 and 200 mm at a temperature of 600°C only differed by about 1% from each other. Indeed the comparison of the shear strength of the specimens which were burned at 900°C, the shear strength differed only by a maximum of 2% between the specimens on the various spacing variations.

Another detected result was a consistent trend of decreasing shear strength when the temperature used during combustion of specimens increased. Nevertheless from the entire specimens, the maximum reduction occuring in shear strength was only 15% to the shear strength of the specimens which were at normal temperature (the specimens were burned at 900°C).

Furthermore, Fig. 11 shows the effect of space stirrups on the shear force relationship to mid-span deflection at various temperatures. Similar to the shear strength behavior described in the paragraph above, the behavior of curves at each observed temperature from zero to approximately 85% of peak forces is relatively coincident with each other although the stirrups spaces used vary from 100, 150 and 200 mm. The maximum shear strength of specimens with each other at one temperature also only differed very little. In the post-peak phase, the curve shows the sloping phase of the specimen which is relatively sloping. Because after the peak response the steel fibers and stirrups contribute to prevent the shear failure of the beam hence it does not collapse suddenly.

4.2.2 Ductility

The ductility ratio of each specimen is shown in Fig. 12, where the stirrups spacing effects (100 mm, 150 mm and 200 mm) were evaluated against the deformation ability of the specimens burned at normal to high temperatures. In general it can be said that reduction the spacing of stirrups will consistently enhance the ductility of the specimens except for specimens which were burned at 300°C, whereas specimens with stirrups of 150 mm spacing have higher ductility values compared to ductility of specimens with installed stirrups of 100 mm spacing.

Ductility specimens seem significantly different if the comparison refers to the temperature effects as shown in Fig. 13 and Table 3 (spacing of constant stirrups). Specimens burned at higher temperatures tend to reduce the ductility of beams. This result shows that in the specimens burned at higher temperatures, the ability of steel fibers and stirrups to resist beam deformation also weaken.

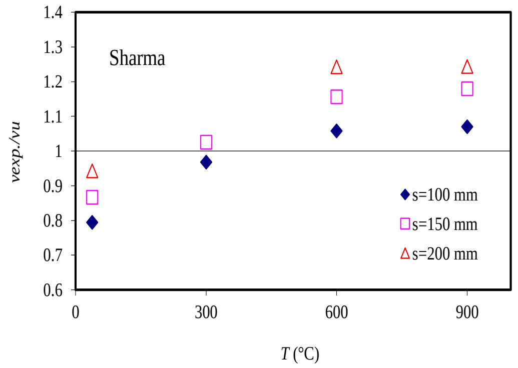

Fig. 14 Comparison of Sharma model with the experimental results

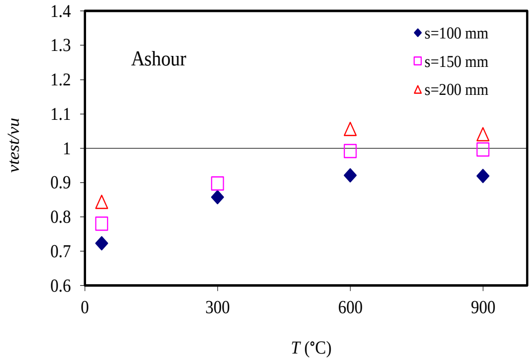

Fig. 16 Comparison of Ashour model with the experimental results

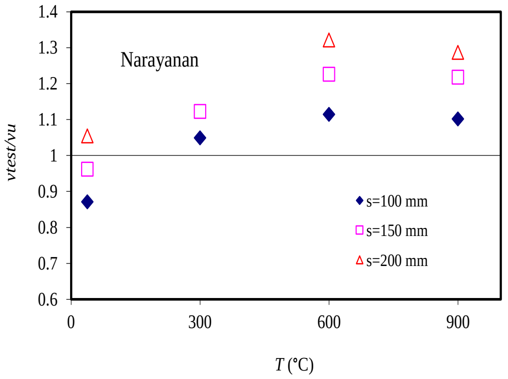

Fig. 15 Comparison of Narayanan model with the experimental results

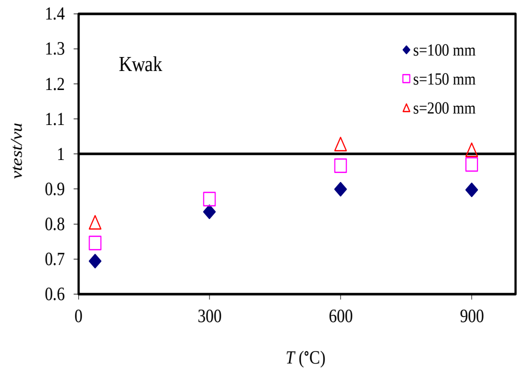

Fig. 17 Comparison of Kwak model with the experimental results

4.3 Comparison with shear strength models

Furthermore the shear strength of above experiment results will be compared with predictions of shear strength along with the models described in Table 1. In the evaluation, the ratio of v_{exp} value to v_u was performed to all specimens. There was a difference of 20% between the shear strength prediction based on the maximum Sharma's model and the experimental results (Fig. 14). At normal temperatures, the prediction of the shear strength of specimens with a-200 mm spaced- stirrups was seen close to the experimental results. However if the specimen is burned at a temperature of 300°C, the predicted shear strength is quite accurate as the beams are installed with a-150 mm spaced stirrup. The accuracy of the Sharma's model looked excellent if the specimens burned at temperatures of 600°C and 900°C, that was in a-100 mm spaced- stirrups mounted beam. Narayanan's model had very good accuracy in predicting experimental results, especially for specimens burned at temperatures of 300°C, 600°C, 900°C and the beams with stirrups spacing 100 mm (Fig. 15).

Shear strength based on Ashour's proposed model differed above 10% from experimental results in control specimens (beams with variations of stirrup spacing 100, 150 and 200 mm), specimens burned at 300°C (beams with stirrups spacing 100 and 150 mm) and specimens post-fuel at temperatures of 600°C and 900°C (beams with 100 mm spacing stirrups) (Fig. 16). The Ashour's model had a difference of under 5% for the experimental results in post-fuel specimens at temperatures of 600°C and 900°C where spacing of stirrups on beams was 150 mm and 200 mm. In addition the prediction results based on Kwak's proposed model on the experimental results showed not much distinctive compared to the evaluation results based on the Ashour's model (Fig. 17).

The results of the comparison among shear strength models and the results of the above experiments have shown that most of the shear strength predictions along with the developed models differed over 10%. This is due to the characteristics of the material used in reducing the shear strength equations that are dismilliar to each other, neither are the characteristics of the material used in this experiment. As known in this experiment there are also additional parameters, namely temperature variations.

5. Conclusions

This paper presents the research of the shear strength and deformation of stirrups mounted beams in post-burned conditions. The general conclusion are follows:

- The failure mode of all specimens is dominated by flexural failure and diagonal tension failure. The flexural failure mode is one of the roles of the presence of steel fibers (0.5%) and stirrups that also functions to prevent shear failure in the beam.
- At each reviewed temperature, stirrups spaced on the

beam did not have a significant effect in determining the beam shear strength.

• In the case of this study the concrete beam containing steel fibre fraction was only 0.5% with a maximum space of 200 mm (1.22*d*) or above the spacing provision based on ACI 318-14 still having optimal shear strength.

• In general, stirrups spacing reduction and temperature reduction imposed on the beam tend to enhance beam ductility.

• The shear strength prediction based on fibrous concrete shear strength models varies with the experimental results, one of them is caused either by difference of mechanical properties or material nature used in developing these models during experiment.

• The results of this study also recommend the need for further research by reviewing broader parameters such as higher steel fibre fractions in order to obtain more general models of shear strength.

Acknowledgment

The research is a part of the results of the Competitive Research Program (*Hibah Bersaing*), Contract No. 002/006.2/PP/SP/2013, funded by the Directorate General of Higher Education, Ministry of Education and Culture, Republic of Indonesia. The support received for this research is gratefully acknowledged.

References

ACI Committee 318 (2014), Building Code Requirements for Structural Concrete (ACI-318-14) and Commentary (318R-14), American Concrete Institute, Farmington Hills, MI.

ACI Committee 544 (1988), "Design considerations for steel fibre reinforced concrete", *ACI Struct. J.*, **85**(5), 1-18.

Antonius, Imran, I. and Setiyawan, P. (2017), "On the confined high-strength concrete and need of future research", *Procedia Eng.*, **171**, 121-130. https://doi.org/10.1016/j.proeng.2017.01.318.

Antonius, Purwanto and Harprastanti, P. (2019), "Experimental study of the flexural strength and ductility of post burned steel fiber RC beams", *Int. J. Technol.*, **10**(2), 428-437.

Antonius, Widhianto, A., Darmayadi, D. and Asfari, G.D. (2014), "Fire resistance of normal and high-strength concrete with contains of steel fibre", *Asian J. Civil Eng.*, **15**(5), 655-669.

Araujo, D. de Lima, Nunes, F.G.T., Filho, R.D.T. and Andrade, M.A.S. (2014), "Shear strength of steel fiber-reinforced concrete beams", *Acta Scientiarum*, **36**(3), 389-397.

Ashour, S.A., Hasanain, G.S. and Wafa, F.F. (1992), "Shear behavior of high-strength fiber reinforced concrete beams", *ACI Struct. J.*, **89**(2), 176-184.

Barros, J.A.O., Lourenco, L.A.P., Soltanzadeh, F. and Taheri, M. (2013), "Steel fibre reinforced concrete for elements failing in bending and in shear", *Adv. Concrete Constr.*, **1**(1), 1-27. http://dx.doi.org/10.12989/acc.2013.1.1.001.

Blesak, L., Goremikins, V., Wald, F. and Sajdlova, T. (2016), "Constitutive model of steel fibre reinforced concrete subjected to high temperatures", *Acta Polytechnica*, **56**(6), 417-424. https://doi.org/10.14311/AP.2016.56.0417.

Gomes, L.D. dos Santos, Oliveira, D.R.C., Neto, B.N. de Moraes, Medeiros, A.B., Macedo, A.N. and Silva, F.A.C. (2018), "Experimental analysis of the efficiency of steel fibers on shear strength of beams", *Lat. Am. J. Solid. Struct.*, **15**(7), 1-16. https://doi.org/10.1590/1679-78254710.

Han, A.L., Antonius and Okiyarta, A.W. (2015), "Experimental study of steel fiber reinforced concrete beams with confinement", *Procedia Eng.*, **125**, 1030-1035. https://doi.org/10.1016/j.proeng.2015.11.158.

Indonesian National Standard (2012), Procedures of Mixed Selection for Normal Concrete, Heavy Concrete and Mass Concrete, SNI 7656:2012. (in Indonesian)

Indonesian National Standard (2013), Requirements of Structural Concrete for Building, SNI 2847-2013. (in Indonesian)

Jain, K. and Singh, B. (2013), "Steel fibres as minimum shear reinforcement in reinforced concrete beams", *Mag. Concrete Res.*, **65**(7), 430-440. https://doi.org/10.1680/macr.12.00113.

Kwak, Y.K., Eberhard, M.O., Kim, W.S. and Kim, J. (2002), "Shear strength of steel fiber-reinforced concrete beams without stirrups", *ACI Struct. J.*, **99**(4), 530-538.

Lim, W.Y. and Hong, S.G. (2016), "Shear tests for ultra-high performance fiber reinforced concrete (UHPFRC) beams with shear reinforcement", *Int. J. Concrete Struct. Mater.*, **10**(2), 177-188. https://doi.org/10.1007/s40069-016-0145-8.

Luo, J.W. and Vecchio, F.J. (2016), "Behavior of steel fiber-reinforced concrete under reversed cyclic shear", *ACI Struct. J.*, **113**(1), 75-84.

Narayanan, R. and Darwish, I.Y.S. (1987), "Use of steel fibers as shear reinforcement", *ACI Struct. J.*, **84**(3), 216-227.

Paultre, P., Eid, R., Langlois, Y. and Lévesque, Y. (2010), "Behavior of steel fiber-reinforced high-strength concrete columns under uniaxial compression", *J. Struct. Eng.*, **136**(10), 1225-1235. https://doi.org/10.1061/(ASCE)ST.1943-541X.0000211.

Ponikiewski, T., Katzer, J., Kilijanek, A. and Kuźmińska, E. (2018), "Mechanical behaviour of steel fibre reinforced SCC after being exposed to fire", *Adv. Concrete Constr.*, **6**(6), 631-643. http://dx.doi.org/10.12989/acc.2018.6.6.631.

Sharma, A.K. (1986), "Shear strength of steel fiber reinforced concrete beams", *ACI J.*, **83**(4), 624-628.

Tadepalli, P.R., Dhonde, H.B., Mo, Y.L. and Hsu, T.T. (2015), "Shear strength of prestressed steel fiber concrete I-beams", *Int. J. Concrete Struct. Mater.*, **9**(3), 267-281. https://doi.org/10.1007/s40069-015-0109-4.

Yoon, Y.S., Yang, J.M., Yoo, D.Y. and Yuan, T.F. (2017), "Replacing stirrups with steel fibers in high-strength concrete beams", *The 2017 World Congress on Advances in Structural Engineering and Mechanics (ASEM 17)*, Korea.

JK